Taylor & Francis
Taylor & Francis Group

RESEARCH ARTICLE

🔓 OPEN ACCESS   Check for updates

Study of immune-tolerized cell lines and extracellular vesicles inductive environment promoting continuous expression and secretion of HLA-G from semiallograft immune tolerance during pregnancy

Kyoungshik Cho 🔸, Hyejin Kook 🔸, Suman Kang 🔸 and Jangho Lee 🔸

R&D Center of Stemmedicare Ltd, Seoul, Republic of Korea

ABSTRACT

An immune reaction is a protector of our body but a target to be overcome for all non-self-derived medicine. Extracellular Vesicles (EVs), noted as a primary alternative to cell therapy products that exhibit immune rejection due to mismatching-major histocompatibility complex (MHC), were discovered to have excellent curative effects through the delivery of various biologically active substances. Although EVs are sure to incur immune reaction by immunogenicity due to alloantigens from their parental cells, their immune rejection is rarely known. Hence, to develop cell lines and EVs as medicines with no immune rejection, we noted the immune tolerance where the foetus, as semiallograft, is perfectly protected from the maternal immune system. We designed the ex-vivo culture systems to simulate in-vivo environmental factors inducing extravillous trophoblast (EVT)-specific Human Leukocyte Antigen-G (HLA-G) expression and secretion of HLA-G-bearing EVs at the mother-foetus interface. Using them, we confirmed that immune-tolerized stem cells (itSCs) continuously expressing and secreting HLA-G like EVTs during pregnancy can be induced. Also, EVs secreted from itSCs are verified as immune-tolerized EVs (itSC-EVs) containing HLA-G and not causing immune rejection through various analytical methods. These findings can provide a new perspective on the local and extensive immune tolerance environment where HLA-G is expressed and secreted by pregnancy-related hormones and different biological conditions. Furthermore, they show the new way to develop itSCs-EVs-based therapeutics that are free from time, space, and donor limitation causing immune rejection.

Abbreviations: CFSE: carboxyfluorescein succinimidyl ester; DC: dendritic cells; ELISA: enzyme-linked immunosorbent assay; EV: extracellular vesicles; EVT: extravillous trophoblast; FSH: follicle stimulating hormone; HA: hyaluronic acid; hCG: human chorionic gonadotropin; HLA-G: human leukocyte antigen G; iPSC: induced pluripotent stem cells; itSC-EVs: immune-tolerized extracellular vesicles from itSCs; itTBC-EVs: immune-tolerized extracellular vesicles from itTBCs; itSCs: immune tolerized stem cells; itTBCs: immune-tolerized trophoblast cells; LH: luteinizing hormone; MHC: major histocompatibility complex; MSC: mesenchymal stem cells; NK: natural killer cells; NTA: nanoparticle tracking analysis; PBMC: peripheral blood mononuclear cells; PHA: phytohemagglutinin; SP-IRIS: single particle interferometric reflectance imaging sensing; STB: syncytiotrophoblast

Introduction

Extracellular vesicles (EVs) are lipid-bilayer particles secreted by all cells and carry out the biological functions including cell regeneration, proliferation, differentiation, apoptosis, immune reaction and angiogenesis through an intercellular transfer of biologically active substances such as proteins, RNAs, enzymes and hormones [1]. Especially mesenchymal stem cells-derived EVs (MSC-EVs) are known to have curative effects on the heart and cardiovascular diseases, liver and kidney damage, neurogenesis, and Alzheimer disease and the immunoregulatory impacts such as reduction of graft-versus-host-disease, survival extension of transplanted organs, and autoimmune diseases [2–8]. For these reasons, EV-bases therapeutics are drawing much attention as "cell-free therapy" to overcome the disadvantages of conventional cell therapy products (i. e., immunogenicity and immune reactions due to mismatching MHC, low engraftment, paracrine effect, tumorigenicity, and donor limitation). On the other hand, although EVs also have immunogenic MHC molecules of parental cells, it is rarely known to have the possibility of causing immune rejection. Donor dendritic cell (DC)-derived exosomes alone can cause an immune reaction by stimulating recipient T cell [9]. And, most of the

intravenously injected exosomes in the mouse model appeared to be eliminated by macrophage [10]. These results demonstrate that EV-based therapeutics must develop a new strategy to escape immune reaction by which allograft cell therapy is still tied up on the verge of commercialization. Although many researchers tried to reduce immune rejection by artificially controlling mis-matching-MHC molecule expression in allograft induced pluripotent stem cells (iPSCs) and MSCs [11–14], there are few studies for lowering immune rejection of allograft EVs.

Hence, we hypothesized that the solution to establish cell- and EV-based medicines without immune reaction is within the bodily process of ovulation, implantation, and pregnancy during which immune response is most entirely and naturally controlled. Trophoblasts, developed from the embryo during ovulation and implantation, secrete HLA-G influenced by pregnancy-related hormones from the pituitary gland, thereby protect the semi-allogeneic foetus from the maternal immune system. In particular, extravil-lous trophoblasts (EVTs) present at the maternal-foetal interface are known to contribute to the maintenance of healthy pregnancy by continuing invasion into the mother's decidua and secretion of HLA-G-containing EVs and soluble HLA-G molecules [15]. Non-classical human leukocyte antigen G class I (HLA-G) is known to induce immune tolerance and control immune reactions to all immune cells (i.e., T cells, natural killer (NK) cells, B cells, dendritic cells (DC), macrophage, and monocyte). It exists as membrane-bound isoform (HLA-G1/2/3/4) or soluble isoforms (HLA-G5/6/7) by alternative splicing during transcription [16]. But trophoblast-restricted HLA-G expression characteristics, detailed formation mechanism, and function of each HLA-G isoforms are not widely known. It is only known that HLA-G, largely HLA-G1 expressed in trophoblast surface, contact with inhibitory receptors of T and NK cells and soluble HLA-G5 secreted by EVTs stimulate differentiation into regulatory T cells and tolerogenic DCs having immunoregulatory character-istics [17–19].

In this study, we set several hypotheses of in vivo environmental factors causing EVT-specific HLA-G expression and secretion at the maternal-foetal inter-face. We devised the ex-vivo culture system to establish immune-tolerized trophoblast cells (itTBCs) like EVTs that can express various HLA-G isoforms and secret soluble HLA-G and HLA-G-containing EVs. We demonstrated to induce itTBCs in the devised ex-vivo culture system and then verified our hypothesis to establish an immune tolerance environment in vitro that can overcome immune rejection. Moreover, we applied the established ex-vivo culture system to HLA-G^{Negative} stem cells. We were able to verify that immune-tolerized Stem Cells (itSCs) could be induced

just as previously produced itTBCs. Finally, we revealed that EVs secreted from itSCs (itSC-EVs) were immune-tolerized EVs able to induce local immune tolerance through membrane-bound HLA-G isoforms expression and extensive immune tolerance by containing soluble HLA-G isoforms. Our results provide new explanations on the immune tolerance mechanism induced by various HLA-G isoforms secreted from EVTs during pregnancy. Furthermore, we propose the possibility of solving immune rejection in organ transplantation and allogeneic cell therapy by itSC-EVs containing HLA-G.

Hypotheses

Hypotheses of environmental factors that induced EVT-specific HLA-G expression and secretion at the maternal-foetal interface

To elucidate the mechanism of immune tolerance by HLA-G that is specifically expressed and secreted by trophoblast during pregnancy, we divided the three environmental factors at the maternal-foetal interface, as shown in Figure 1(a). (i) Promoting HLA-G gene transcription by pregnancy-related hormones; (ii) Promoting HLA-G protein expression and secretion activating invasion and proliferation of EVTs; and (iii) Promoting the expression and secretion of various HLA-G isoforms. We set the hypotheses for each fac-tor, as shown in Figure 1(b). To verify them, we imple-mented an ex-vivo culture system similar to the maternal-foetal interface (HA-Matrix^{Decidua}) and intended to prove them through the flowchart, as shown in Figure 1(c).

Hypothesis 1. Temperature factor triggering EVT-specific HLA-G transcription by progesterone and hCG

To date, the HLA-G transcription mechanism restricted to trophoblast in healthy conditions has not been ultimately revealed. But, in HLA-G unique pro-moter region, regulatory factors such as ISRE (inter-feron-stimulated regulatory element), HSE (heat-shock element), HRE (Hypoxia response element), PRE (pro-gesterone response element), particularly distinguished from other HLA Class I, are known to exist [20]. Here, we focused on progesterone secreted continuously dur-ing implantation and pregnancy as a transcriptional promoter of trophoblast-specific HLA-G gene. However, there are limitations to implement in vitro the complex mechanism of hormone secretion
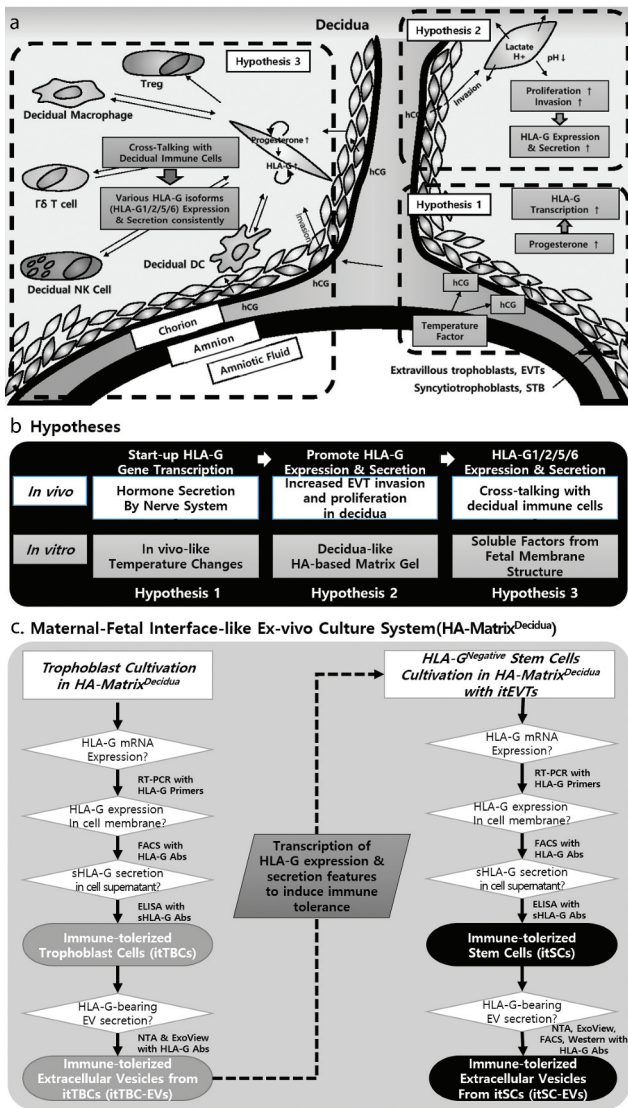
Figure 1. Conceptual frameworks for hypotheses of environmental factors inducing immune tolerance by HLA-G during pregnancy and the verification procedure using Ex-vivo Culture System. (a) In vivo Environmental factors for promoting HLA-G gene transcription, various HLA-G isoforms expression, and secretion consistently. (b) Hypotheses that encourage EVT-specific HLA-G transcription, sustained HLA-G1/2 expression and soluble HLA-G5/6 secretion at the maternal-foetal interface during pregnancy and in vitro culture conditions for demonstrating them. (c) Flowchart for verification of hypotheses by inducing immune-tolerized Stem Cells (itSCs) and immune-tolerized EVs (itSC-EVs) secreted from them using maternal-foetal interface-like ex-vivo culture system (HA-Matrix^Decidua).

regulated by the nervous system. Instead, we noted that the secretion patterns of female hormones are strictly related to changes in women's body temperature consistent in the menstruation-ovulation-fertilization-implantation-pregnancy process. In Supplemental Figure 1(b), the rapid change in body temperature before and after the ovulation seems to induce the

secretion of progesterone in the body. So, we assumed that in vitro culture conditions with the temperature change similar to that in women's body would be a trigger for the induction of progesterone and human chorionic gonadotropin (hCG), a promotor of progesterone secretion, in trophoblast by replacing the nervous system (Supplemental Figure 1D).

Hypothesis 2. Physiochemical factors promoting HLA-G secretion by a matrix that provides a decidual-like environment stimulating EVTs proliferation and invasion

EVTs at the maternal-foetal interface continue to invade into the decidua and secrete soluble HLA-G and HLA-G-containing EVs. In this process, EVTs carry out aerobic glycolysis appropriate for proliferation and differentiation activated by hCG [21]. Therefore, we hypothesized that decidual-like physical environment capable of sustaining EVTs invasion and proliferation, and low pH chemical environment appropriate for energy metabolism properties of EVTs, might promote expression and secretion of HLA-G proteins in EVTs (Figure 1(a)). To demonstrate this, among various biocompatible polymers, we designed a hyaluronic acid (HA)-based matrix to provide the decidual-like physicochemical environment suitable for invasion and proliferation of EVTs in the ex-vivo culture system.

Hypothesis 3. Physiological factors inducing the expression and secretion of various HLA-G isoforms from EVTs through cross-talking with decidual immune cells

Unlike other subpopulations of trophoblasts in foetal tissues secreting only HLA-G5, EVTs in maternal decidua can express and secrete HLA-G1, -G2, -G5 and -G6 [22]. From this, we assumed that various HLA-G isoforms would induce an immune tolerant environment that completely protects the foetus from the mother's immune system. As a physiological factor causing this, we focused on cross-talking with EVTs and decidual immune cells that do not exist in foetal tissue but only in the maternal decidua. However, it is impossible to establish a co-cultivation system with all decidual immune cells in vitro. So, we attempted to implement this by simulating the foetal membrane structure, as shown in Figure 1(a). Since the foetus is present in amniotic fluid surrounded by the amniotic membrane, we co-cultured the amniotic membrane (hAM-MSCs) and amniotic fluid stem cells (hAF-MSCs) on a multi-plate similar to the foetal membrane

structure. Protein Analysis of the co-culture supernatant has shown that it contains the optimal ratio of pregnancy-related hormones such as hCG and LH as well as various immunosuppressive soluble factors that were assumed to be secreted by decidual immune cells. From these results, we tried to apply the EV-enriched solution obtained through the co-culture of hAM-MSCs and hAF-MSCs (AF/AM-MSC^{CO}-EVs) to the HA-based matrix of Hypothesis 2.

Establishment of maternal-foetal interface-like ex-vivo culture system promoting continuous expression and secretion of various HLA-G isoforms from Trophoblast

We established ex-vivo culturing systems to verify EVT-specific temperature, physicochemical, biological hypotheses for promoting sustained expression and secretion of various HLA-G isoforms at the maternal-foetal interface. First, among diverse trophoblast cell lines, we selected BeWo cell line. It has substantially lower HLA-G expression in comparison to JEG-3 cell line, a typical HLA-G-positive EVT, and has both characteristics of hCG-secreting syncytiotrophoblast (STBs) and decidua-invading EVTs [23]. Also, by mixing AF/AM-MSC^{CO}-EVs with hyaluronic acid (Sigma-Aldrich) providing a decidual-like physicochemical environment, we prepared a matrix for in vitro trophoblast cultivation (HA-Matrix^{Decidua}). Finally, we have completed the ex-vivo culture system by applying the temperature condition similar to body temperature change and the circulation condition (Supplemental Figure 2).

And we investigated whether BeWo cells cultured in HA-Matrix^{Decidua} express and secrete various HLA-G isoforms like EVTs only at the maternal-foetal interface during pregnancy. We also investigated where these cells secrete HLA-G-containing EVs. Also, we demonstrated the formation of the HLA-G-specific homodimer that has a much higher binding affinity with the immune cell's inhibitory receptors than the monomer [24,25]; with these, we confirmed our hypotheses.

Materials and methods

Cell lines and culture

Human trophoblast cells BeWo and their culture medium were purchased from ATCC (Manassas, VA, USA). BeWo cells were cultured in F-12k medium (ATCC) supplemented with 100 U/mL of penicillin (Sigma-Aldrich, St. Louis, MO, USA), 100 μg/mL of streptomycin (Sigma-Aldrich) and 10% foetal bovine serum (FBS) (Gibco by Thermo Fisher Scientific, Waltham, MA, USA). Human amniotic fluid-derived mesenchymal stem cells (hAF-MSC) were obtained from the healthy donor with written informed consent and approved by the Institutional Bioethics Committee of Stemmedicare Ltd. (No.1–2019111903-B-N-01) for utilization of tissues and all experimental procedures. Human Amniotic Mesenchymal stem cells (hAM-MSC) and human umbilical mesenchymal stem cells (HU-MSC) were purchased from ScienCell (Carlsbad, CA, USA). These MSCs were maintained in DMEM medium (Welgene, Republic of Korea) supplemented with 100 U/mL of penicillin (Sigma-Aldrich), 100 μg/mL of streptomycin (Sigma-Aldrich) and 10% heat-inactivated foetal bovine serum.

All the cells were cultured on specially designed HA-Matrix^{Decidua} with in vivo-like temperature change and circulation conditions in a 5% CO_2. In addition, the control groups of each cell were typically cultured in a 2D-culture plate in a 5% CO_2 humidified atmosphere at 37℃.

In vivo-like temperature change and circulation conditions

An in vivo-like culture condition for inducing immune-tolerized cell lines was established using temperature change and vibration conditions. The temperature change profile was applied to promote progesterone and hCG secretion for stimulating HLA-G production from immune-tolerized cells. Cell culture temperature was changed between 36.0 ℃ and 37.0 ℃ with a five or six-day cycle as shown in Supplemental Figure 1(d) during each subculture. At the same period, these cells were cultured in a shaking incubation system providing a circulation condition with 1 24-hr cycle, as shown in Figure 3(d), to facilitate the signal transduction between the in vitro culture matrix gel and immune-tolerized cells and promotes autocrine of progesterone and various soluble factors that sustain the HLA-G expression and secretion.

Establishment of co-culture system of hAF-MSCs and hAM-MSCs

An indirect co-culture system of hAF-MSCs and hAM-MSCs was established using a multi-dish with polycarbonate membrane insert (Thermo Fisher Scientific). hAM-MSCs were seeded at a density of 2 x 10^4/cm^2 in 6-well plate and hAF-MSCs were seeded at a density of 2 x 10^4/cm^2 in a 0.4 μm pore insert (Nunc). After that, they were cultured in DMEM serum-free medium in a 5% CO_2 humidified atmosphere at 37℃ for 120 hrs to obtain the conditioned medium.

Reverse transcription polymerase chain reaction (RT-PCR)

Total RNA was prepared from the cells using TRIzol according to the manufacturer's instructions (Invitrogen by Thermo Fisher Scientific, Waltham, MA, USA). A total of 1 μg of DNase-treated RNA was transcribed into cDNA using 200 units of Superscript II reverse transcriptase (Invitrogen) and 150 ng of random primers (Invitrogen). The sequences of the primers for HLA-G isoforms are listed in Supplemental Table 1. All PCR samples were analysed by electrophoresis on 2% agarose gel (Amresco, Solon, OH, USA) that contained 0.5 μg/ml ethidium bromide (Sigma-Aldrich).

Flow cytometry

The expression of HLA-G proteins and specific markers in BeWo cells, MSCs, and EVs from these cells were quantified by flow cytometry. The cells were harvested and stained with anti-Human CD24 FITC (eBioscience by Thermo Fisher Scientific, Waltham, MA, USA), anti-Human CD90 PE (BioLegend), anti-Human CD105 PE (BioLegend), anti-HLA-G MEM-G/9 FITC (Invitrogen), and anti-HLA-G 4H84 Alexa Fluor 488 (Novus Biologicals, Centennial, CO, USA) antibodies for 40 min at 4°C. The EVs were stained with anti-Human CD9 APC (eBiosience), anti-Human CD63 PE (eBiosience), and CD81 FITC (Invitrogen) antibodies for 40 min at 4°C. Then, the cells and EVs were detected by flow cytometry. For the detection of EVs, various sizes of reference-beads (Thermo Fisher Scientific) were used. The data were analysed by Flowjo software.

The PBMCs were stained with anti-Human CD3 APC (Invitrogen) and anti-Human CD25 FITC (Invitrogen). $CD3^+/CD25^-$ and $CD3^+/CD25^+$ cells were considered T effector cells and T_{reg} cells, respectively. Results were calculated using the GraphPad Prism software version No. 8 (San Diego, CA, USA).

Table 1. The concentration of proteins in AF/AM-MSC^{CO}-EVs promoting continuous HLA-G expression and secretion in EVTs.

Proteins	Concentration (pg/ml)	
	In small EVs (0.22-μm filter)	In medium EVs (0.45-μm filter)
IL-1β	4.6 ± 0.6	8.2 ± 3.0
IL-10	6.4 ± 0.0	8.1 ± 1.7
TNF-α	41.65 ± 1.65	58.6 ± 18.6
TGF-β	2,127.4 ± 362.9	2,350.1 ± 140.2
IFN-γ	7.5 ± 1.1	12.05 ± 3.45

Western blot assay

The expression of soluble HLA-G in EVs was detected by western blotting. The HLA-G protein was extracted from EVs, using Trichloroacetic acid (TCA, Sigma-Aldrich) precipitation. HLA-G was separated on 10% SDS-polyacrylamide gels. After electrophoresis of protein extracted from the EVs, the protein was transferred onto a polyvinylidene difluoride membrane and probed with primary anti-HLA-G 5A6G7 antibody (Abcam, Cambridge, UK) ad HRP-conjugated secondary goat anti-mouse IgG antibody (Abcam). The expression level of each isoform of HLA-G protein was detected by the ECL solution kit (Thermo Fisher Scientific) and Chemiluminescence Imaging System (Alliance Mini HD9, UVITEC, Cambridge, UK).

Enzyme-linked immunosorbent assay (ELISA)

The concentrations of HLA-G, soluble HLA-G, Progesterone, and hCG in the samples, were detected by Human HLA-G ELISA Kit (LSBio, Seattle, WA, USA) using MEM-G/9 antibody, soluble HLA-G ELISA Kit (MyBioSource, San Diego, CA, USA) using 5A6G7 antibody, Progesterone ELISA Kit (Elabscience, Houston, TX, USA) and hCG ELISA Kit (Abcam) respectively according to the manufacture's instruction.

Antibody array

The protein profiles secreted from MSCs were analysed by Antibody Array Assay Kit (Full Moon Biosystems, Sunnyvale, CA, USA) according to the manufacturer's instruction.

EVs preparation

Multi-stage filtration

To increase the efficiency of the subsequent stage filtration and recovery a high yield of EVs, multi-stage filtration method was applied (Supplemental Figure 3A). The cell culture supernatant, centrifuged at 1,500 RPM for 5 min, was filtered with a 0.8-μm filter to remove cell debris and apoptotic bodies completely, and the supernatant was filtered with a 0.45-μm filter twice. At the first filtration, we filtered less than half the sample volume of the supernatant recommended by the manufacturer, and through the second filtration of the collected filtrates, we got small/medium EVs used in the preparation of Matrix for ex-vivo culture system. To obtain small EVs, we filtered the supernatant with a 0.22-μm filter in the same manner above.

AF/AM-MSC^{CO}-EVs

The conditioned medium obtained from serum-free co-cultivation of hAM-MSCs and hAF-MSCs in multi-dish plate was centrifuged at 1,500 RPM for 5 min at the room temperature, and the supernatant was filtered with a 0.45-μm filter after multi-stage filtration to obtain AF/AM-MSC^{CO}-EV-enriched solution.

itTBC-EVs

The conditioned medium, obtained from serum-free cultivation of immune-tolerized trophoblast cells (itTBCs) with a seeding density of 2.0 x 10^4/cm^2 in HA-Matrix^{Decidua} with in vivo-like temperature change and circulation condition, was centrifuged at 1,500 RPM for 5 min at the room temperature, and the supernatant was filtered with a 0.45-μm filter after multi-stage filtration to obtain itTBC-EVs.

itSC-EVs

The conditioned medium, obtained from serum-free cultivation of immune-tolerized stem cells (itSCs) with a seeding density of 2.0 x 10^4/cm^2 alone without any Matrix after washing with PBS several times to remove any contaminant during the cultivation on HA-Matrix^{Decidua} containing itTBC-EVs with in vivo-like temperature change and circulation condition, was centrifuged at 1,500 RPM for 5 min at the room temperature, and the supernatant was filtered with a 0.22-μm filter after multi-stage filtration to obtain itSC-EVs.

NTA measurement of EVs with Nanosight NS300

The concentration and size of EVs were analysed by NTA using a NanoSight NS300 with a Blue 488 nm laser (Malvern Panalytical, Malvern, UK). All samples were diluted in PBS to reach concentrations inside the precision range of the NTA machine (2×10^8 to 10×10^8 particles/ml). EVs were measured at camera level 14 (camera shutter speed: 31.48 shutters/ms, slider gain: 366). After capture, the videos have been analysed using the in-build NanoSight Software NTA 3.4 Build 3.4.003 with a detection threshold 5.

Protein analysis of EVs

Protein content of AF/AM-MSC^{co}-EVs was determined by BCA protein assay (Thermo Fischer Scientific). The concentration of human growth factors and cytokines were analysed by Quantibody Human Cytokine Array 1000 (RayBiotech, Peachtree Corners, GA, USA) according to the manufacturer's instruction.

EV analysis with ExoView^{TM} R100

Co-Expression of CD9, CD61, CD81 and HLA-G in itTBC-EVs and itSC-EVs was analysed by Tetraspanin custom Kit with ExoView^{TM} R100 (NanoView Biosciences, Boston, MA, USA). All samples were diluted in D.W. and incubated on the ExoView Tetraspanin Chip (EV-TC-TTS-01) placed in a sealed 24-well plate for overnight at room temperature. The chips were then washed three times in 1 mL D.W for 3 min. Then, chips were incubated with ExoView Tetraspanin Labelling ABs (EV-TC-AB-01) that consist of anti-CD81 Alexa-555, anti-CD63 Alexa-488, anti-CD9 Alexa-647 and anti-HLA-G MEM-G/9 APC, anti-HLA-G 4H84 Alexa Fluor 488 antibodies. The ExoView Tetraspanin Labelling ABs were diluted 1:100 in D.W. The chips were incubated with 250 μL of the labelling solution for 1 h. The chips were then washed in D.W and dried. The chips were then imaged with the ExoView R100 reader using the ExoScan 2.5.5 acquisition software. The data were then analysed using ExoViewer 2.5.0 with sizing thresholds set to 50 to 200 nm diameter.

T-cell proliferation & T$_{reg}$-cell differentiation assay

The potential for induction of immune tolerance of itSC-EVs was evaluated by T cell proliferation assay and Treg cell differentiation assay. Peripheral Blood Mononuclear Cells (PBMCs) were obtained from the healthy donor with written informed consent and approved by the Institutional Bioethics Committee of Stemmedicare Ltd. for utilization of blood sample and all experimental procedures. In 96-well flat-bottom microplate (Thermo Fisher), 5×10^5 CFSE (Thermo Fisher) pre-labelled PMBCs were seeded per well with MSC^{Control}-EVs (EVs from 5×10^5 MSC^{Control}) and MSC$^{Matrix+T/V}$-EVs (EVs from 5×10^5 MSC$^{Matrix+T/V}$) in a total volume of 200 μL, respectively. The assay medium was RPMI-1640 medium (Sigma-Aldrich) supplemented with 100 U/mL of penicillin (Sigma-Aldrich), 100 μg/mL of streptomycin (Sigma-Aldrich) and 10% heat-inactivated foetal bovine serum. T-cell proliferation and T$_{reg}$-cell differentiation were examined either in the presence of 5 μg/ml of PHA (Sigma-Aldrich) for 5 days. The number of fluorescent cells for untreated and each treatment group was quantitated by Flow Cytometry.

Statistical analysis

Statistical analyses were performed using the Student's t-test, or Mann Whitney test for the comparison of means in more than two groups. Date presented are

mean±S.D. and $P < 0.05$ was considered statistically significant.

Results

Characterization of AF/AM-MSC^{CO}-EVs

Co-culture supernatant of AM-MSC with AF-MSC were centrifuged at low speed to remove cell debris, then AF/AM-MSC^{CO}-EV were collected by multi-stage filtration. Their size and concentration were determined by NTA (n = 3). The concentrations varied between individual preparations ranging from $2.17 \times 10^9 \pm 2.85 \times 10^7$ EVs/ml obtained from 1.0×10^5 MSCs, approximately (Figure 2(a)). The AF/AM-MSC^{CO}-EVs size distribution profiles of the 3 samples were similar and AF/AM-MSC^{CO}-EVs between 50 and 440 nm were detected. The average modal size (defined as the most frequently occurring EV size) of AF/AM-MSC^{CO}-EVs was 143.1 ± 9.1 nm
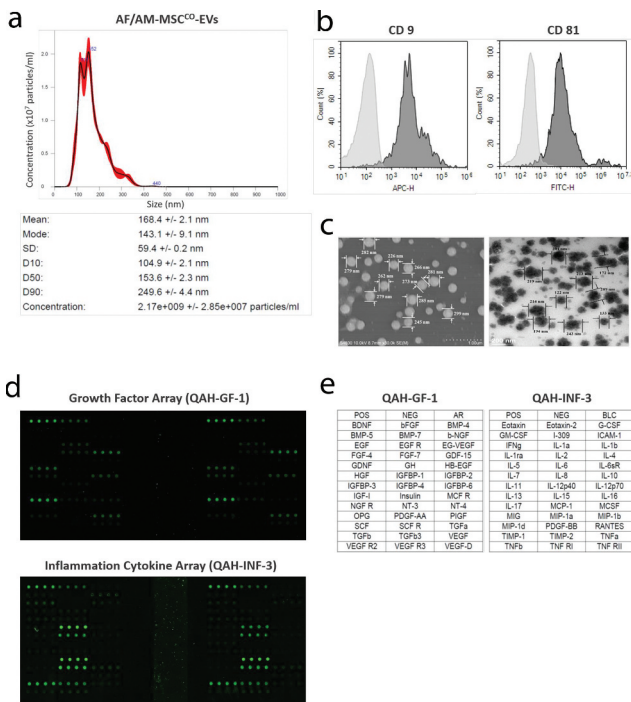
and the average mean size of AF/AM-MSC^{CO}-EVs was 168.4 ± 2.1 nm. The total protein concentration of AF/AM-MSC^{CO}-EV was 423.2 ± 36.2 µg/ml by BCA Pierce Protein Assay Kit (Thermo Fisher Scientific). Figure 2 (b) shows the images of AF/AM-MSC^{CO}-EVs with a scanning electron microscope (SEM) and a transmission electron microscope (TEM), respectively. Exosomal markers (CD9 and CD81) expression were analysed by flow cytometry (Figure 2(c)). The human growth factor and cytokine analysis of AF/AM-MSC^{CO}-EVs was performed by Quantibody® Human Cytokine Antibody Array 1000. Most kinds of growth factors and cytokines were detected (Figure 2(b,c)), especially TGF-β with high concentration. The concentration of specific proteins known to secrete from the decidual immune cells and assumed to promote sustained HLA-G expression and secretion in EVTs were shown in Table 1. As shown in Table 1, the concentrations of specific proteins in medium EVs were higher than those in small EVs. So, we have used AF/AM-MSC^{CO}-EVs obtained by 0.45-µm filter.

Characterization and evaluation of HLA-G expression and secretion of cultured BeWo cells on the hyaluronic acid-based matrix containing AF/AM-MSC^{CO}-EV

To find the optimal condition of hyaluronic acid (HA)-based culture matrix containing AF/AM-MSC^{CO}-EVs for the proliferation of BeWo cells, we prepared various concentrations of HA mixed with AF/AM-MSC^{CO}-EV-enriched solution. According to cell proliferation assay during several subcultures of BeWo cells on the HA-based matrix, the proliferation rate of BeWo cells was proportional to HA concentration in the matrix. But above specific levels, BeWo cell proliferation and recovery were very difficult because the matrix was too sticky. So, we determined the optimal HA concentration mixed with AF/AM-MSC^{CO}-EV-enriched solution showing the highest proliferation rate and recovery rate (HA-Matrix^{Decidua}).

Figure 3(a) is a schematic diagram showing that BeWo cells cultured in HA-Matrix^{Decidua} are the immune-tolerized trophoblast cells (itTBCs) that secrete and express various HLA-G isoforms. Figure 3 (b) shows microscopic images of BeWo cells on the 1st and 6th day after cultivation on HA-Matrix^{Decidua}. We could confirm that they are similar to the proliferative characteristics of general BeWo cells that grow in clusters over time. Figure 3(c) represents the vibration condition of 24-hour-cycle to promote the circulation of soluble factors during BeWo cell cultivation.

Figure 2. Characterization of AF/AM-MSC^{CO}-EVs. (a) Particle concentration and distribution of AF/AM-MSC^{CO}-EVs by Nanosight particle tracking system. (b) FACS analysis of AF/AM-MSC^{CO}-EVs to investigate the expression of exosomal markers (CD9 and CD81). (c) Field Emission Scanning Electron Microscope (FE-SEM, left) and Field Emission Transmission Electron Microscope (FE-TEM, right) images of AF/AM-MSC^{CO}-EVs, respectively. (d) Human growth factor and cytokine array of AF/AM-MSC^{CO}-EVs. The upper and lower panel show the scan images of 40 kinds of human growth factors array (QAH-GF-1) and human cytokine array (QAH-INF-3) of AF/AM-MSC^{CO}-EVs, respectively. (E) The left and right panel represent the list of human growth factors and cytokines on each array.
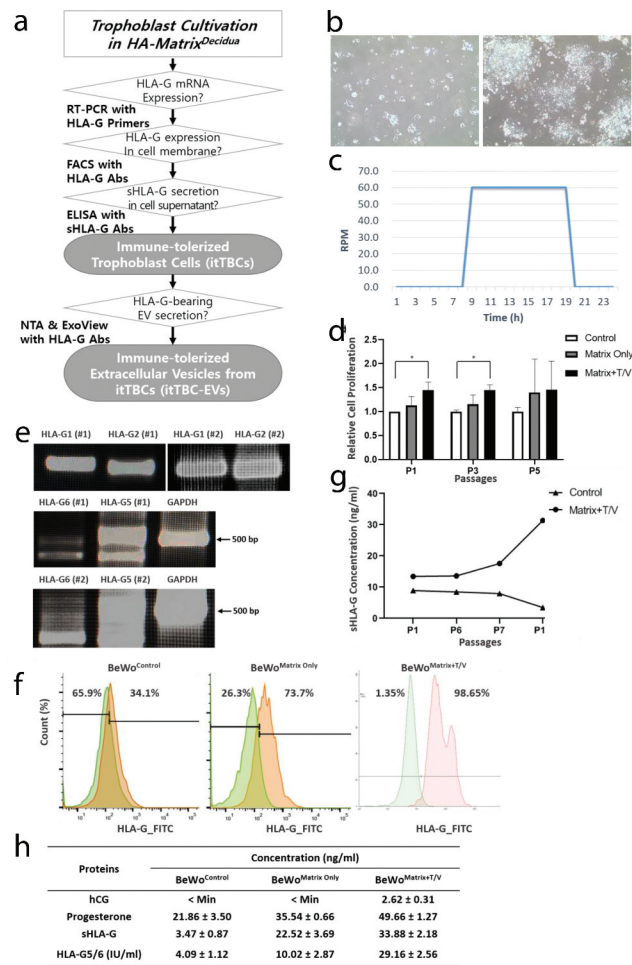
Figure 3. Proliferation and evaluation of HLA-G expression and secretion of cultured BeWo Cells on the HA-Matrix^{Decidua} containing AF/AM-MSC^{CO}-EV with in vivo-like temperature change and circulation conditions. (a) A scheme of verification procedure for induction of immune-tolerized trophoblast cells (itTBCs) and immune-tolerized EVs (itTBC-EVs). (b) Microscope images of cultured BeWo cells on the HA-Matrix^{Decidua}, at the 1st day (left) and 6th day (right) after cultivation. (c) A graph of 24-hour-cyclic vibration condition during BeWo cells cultivation to promote the circulation of various soluble factors between BeWo cells and the HA-Matrix^{Decidua}. (d) Relative cell proliferation assay of BeWo cells cultured on the 2D-culture plate (Control), on the HA-Matrix^{Decidua} without temperature/vibration conditions (Matrix Only), and on the HA-Matrix^{Decidua} under temperature/vibration conditions (Matrix+T/V). Error bars represent SD. *, P < 0.05; Mann Whitney test. (E) Intracellular HLA-G mRNA isoforms expression of BeWo cells cultured on the HA-Matrix^{Decidua} under temperature/vibration conditions (BeWo$^{Matrix+T/V}$) was shown by RT-PCR analysis, with *GAPDH* as a positive control, using designed HLA-G primer set listed in Supplemental Table 1. All HLA-G mRNA isoforms (HLA-G1, G2, G5, and G6) were expressed. (F) FACS analysis of membrane-bound HLA-G expressions on the surface of BeWo^{Control}, BeWo$^{Matrix Only}$, and BeWo$^{Matrix+T/V}$ cells obtained at passage 12 using MEM-G/9 antibody. Two peaks in HLA-G positive BeWo$^{Matrix+T/V}$ cells were generated due to the more colony generation while more active cell proliferation in the ex vivo culture system (Supplemental Figure 4). (g) The concentrations of sHLA-G in the culture supernatant of BeWo$^{Matrix+T/V}$ and BeWo^{Control} cells using MEM-G/9 antibody bound to sHLA-G1 and HLA-G5. (h) Specific proteins quantification contained in the culture supernatant of BeWo^{Control}, BeWo$^{Matrix Only}$, and BeWo$^{Matrix+T/V}$ by ELISA. Each EVs were obtained at passage 12 of each cultivation.

As previously established hypotheses, we applied the temperature change with a five or six-day cycle, as shown in Supplemental Figure 1(d), and the vibration condition to investigate the effects of these conditions on the proliferation of BeWo cells. As a result, we confirmed that the growth rate of BeWo cells cultured in HA-Matrix^{Decidua} with temperature/vibration conditions (BeWo$^{Matrix+T/V}$) is much higher than not only that of BeWo cells cultured in the general culture plate without temperature/vibration conditions (BeWo^{Control}), but also that of BeWo cells cultured in HA-Matrix^{Decidua} without temperature/vibration conditions (BeWo$^{Matrix Only}$) as the subculture progressed (Figure 3(d)). These results are due to the characteristic of EVTs proliferating along with continuous infiltration into the maternal decidua, which shows that HA-Matrix^{Decidua} can provide an optimal physical environment similar to the decidual layer suitable for the invasion of BeWo cells in vitro.

To investigate the intracellular expression of various HLA-G mRNA isoforms in BeWo$^{Matrix+T/V}$, we designed the primer sets of each HLA-G isoforms, HLA-G1, G2, G5, and G6, respectively. As a result of PCR analysis, we verified that all HLA-G mRNA isoforms were expressed (Figure 3(e)) in the lysate of BeWo$^{Matrix+T/V}$ obtained at passage 12. Also, we performed flow cytometry using the MEM-G/9 HLA-G antibody to investigate the expression of membrane-bound HLA-G in BeWo^{Control}, BeWo$^{Matrix\ Only}$, and BeWo$^{Matrix+T/V}$ obtained at passage 12, respectively. Compared with BeWo$^{Matrix\ Only}$ and BeWo^{Control}, it was confirmed that HLA-G isoform was much higher in the cell membrane of BeWo$^{Matrix+T/V}$ (Figure 3(f)). Besides, the sHLA-G concentration (sHLA-G1 shedded from the surface and soluble HLA-G5 secreted from the cells) was measured by ELISA in each culture supernatant collected during the subculture of BeWo cells, respectively. As a result, the concentration of sHLA-G in the culture supernatant of BeWo$^{Matrix+T/V}$ was increased as the subculture progressed, but that of BeWo^{Control} was gradually decreased (Figure 3(g)). Furthermore, ELISA analysis revealed that the culture supernatant of BeWo$^{Matrix+T/V}$ contained progesterone that promotes HLA-G expression and secretion, and hCG that supports continuous progesterone autocrine with a higher level than those of BeWo^{Control} and BeWo$^{Matrix\ Only}$ (Figure 3(h)).

The hypotheses that we established to simulate the bioenvironment during pregnancy, such as HA-Matrix^{Decidua} containing AF/AM-MSC^{CO}-EVs and in vivo-like temperature change and circulation culture conditions, were tested in vitro. From our findings, we verified all hypotheses to promote proliferation and sustained expression and secretion of various HLA-G isoforms from BeWo$^{Matrix+T/V}$. Namely, we demonstrated that the immune-tolerized trophoblast cells (itTBCs), having the ability to continuously express and secrete various HLA-G protein isoforms as like at the maternal-foetal interface during pregnancy, can be established by in vitro culture conditions implemented herein.

Characterization of EVs (itTBC-EVs) from cultivation of immune-tolerized trophoblast cells (itTBCs) on the HA-Matrix^{Decidua} with in vivo-like temperature profile and circulation conditions

Culture supernatant of itTBCs were centrifuged at low speed to remove cell debris, then itTBC-EVs were collected by multi-stage filtration. Their size and concentration were determined and compared with EVs from BeWo^{Control} by NTA (n = 3). The concentrations of BeWo^{Control}-EVs varied between individual

preparations ranging from $5.66 \times 10^8 \pm 1.05 \times 10^7$ particles/ml obtained from 1.0×10^5 BeWo^{Control} approximately (Figure 4(a)), and that of BeWo$^{Matrix+T/V}$ were $1.49 \times 10^9 \pm 2.47 \times 10^8$ particles/ml obtained from 1.0×10^5 BeWo$^{Matrix+T/V}$ approximately, much higher than BeWo^{Control}-EVs (Figure 4(b)). The BeWo-EVs size distribution profiles of each 3 samples were similar each other. But, BeWo^{Control}-EVs between 60 and 680 nm were detected, while BeWo$^{Matrix+T/V}$-EVs between 50 and 450 nm were detected. The average modal size and the average mean size of BeWo^{Control}-EVs were 100.8 ± 5.5 nm and 168.4 ± 2.1 nm, respectively. While, the average modal size and the average mean size of BeWo$^{Matrix+T/V}$-EVs were 100.9 ± 3.1 nm and 125.4 ± 2.4 nm, respectively, rather smaller than BeWo^{Control}-EVs. The concentration of total proteins of BeWo$^{Matrix+T/V}$-EVs was 722.1 ± 88.6 µg/ml through BCA protein assay, rather higher than BeWo^{Control}-EVs (627.6 ± 44.6 µg/ml). The concentrations of specific proteins known to secrete from the EVTs and assumed to promote sustained HLA-G expression and secretion in BeWo^{Control}-EVs, BeWo$^{Matrix\ Only}$-EVs, and BeWo$^{Matrix+T/V}$-EVs (itTBC-EVs) are shown in Table 2. As presented in Table 2, the concentrations of all proteins in itTBC-EVs were much higher than other EVs samples, especially hCG was not detected in BeWo^{Control}-EVs and BeWo$^{Matrix\ Only}$-EVs. In addition, the concentrations of each protein in itTBC-EVs obtained by 0.45-µm filter were higher than those in itTBC-EVs obtained by 0.22-µm filter (Supplemental Table 2), similar to the results in Figure 3(h).

Figure 4(c) shows the images of BeWo$^{Matrix+T/V}$-EVs with a scanning electron microscope (SEM) and a transmission electron microscope (TEM), respectively. We analysed the exosome markers and HLA-G protein markers expressed in each EVs membrane by Exoview device. Figure 4(d) shows the exosomal markers, CD9, CD63, and CD81, expression on BeWo$^{Matrix+T/V}$-EVs, very similar to BeWo^{Control}–EVs. In addition, we verified that the expression of HLA-G markers, 4H84 binding with α1 domain of HLA-G heavy chain to detect all HLA-G isoforms and MEM-G/9 to detect β2m-associated HLA-G isoforms (HLA-G1 and HLA-G5), were much higher in BeWo$^{Matrix+T/V}$-EVs (the right panel of Figure 4(e)) than in BeWo^{Control}-EVs (the left panel of Figure 4(e)). Comparing the EV spots captured with CD9 antibody among the exosomal markers, it was also confirmed that the EV spots (blue and red spots) bound to the HLA-G antibodies were much found in BeWo$^{Matrix+T/V}$-EVs (the right panel of Figure 4(f)) than in BeWo^{Control}-EVs (the left panel of Figure 4(f)). To date, no specific antibodies specifically binding to HLA-G2 have not been developed, so our

Proteins	Concentration (ng/ml)		
	BeWo^Control^-EVs	BeWo^Matrix Only^-EVs	itTBC-EVs**
Progesterone	7.74 ± 0.96	13.51 ± 0.48	21.85 ± 3.49
sHLA-G*	8.79 ± 0.91	15.17 ± 0.48	29.18 ± 1.29
HLA-G5 & HLA-G6 (IU/ml)	26.74 ± 5.88	44.60 ± 0.22	89.74 ± 0.56
hCG	< Min	< Min	1.69 ± 0.07

*: soluble HLA-G1 & HLA-G5
**: The concentrations of each protein in itTBC-EVs obtained by 0.45-μm filter were higher than those in itTBC-EVs obtained by 0.22-μm filter (Supplemental Table 2).

results could not be confirmed accurately. However, the much higher expression of 4H84-single positive-spots (β2m-free HLA-G1 or G2) and 4H84-MEM-G/9-double positive spots indicates that both HLA-G1 and HLA-G2 are present on the itTBC-EVs membrane.

From these findings, itTBC-EVs expressed both membrane-bound HLA-G1 and G2 on the EV membrane and contained both soluble HLA-G5 and G6. It was confirmed that it contains hCG and progesterone that promote HLA-G expression and secretion. Then, we devised a method to induce immune-tolerated stem cell lines (itSCs) from MSCs (HLA-G^Negative^-MSCs), which are known not to express and secrete HLA-G. Initially, we tried to induce itSCs using the co-cultivation system of itTBCs and HLA-G^Negative^-MSCs, as shown in the right pathway of Figure 4(g). Eventually, it succeeded in producing itSCs having immune-tolerant properties capable of secreting and expressing various HLA-G isoforms such as itTBCs (data not shown). However, the co-cultivation method was somewhat unsuitable for future expansion to mass production technology. In the end, we finally designed a new ex-vivo culture system by adding the optimal concentration of itTBC-EVs to the established Matrix^Decidua^, as shown in the left pathway of Figure 4(g).
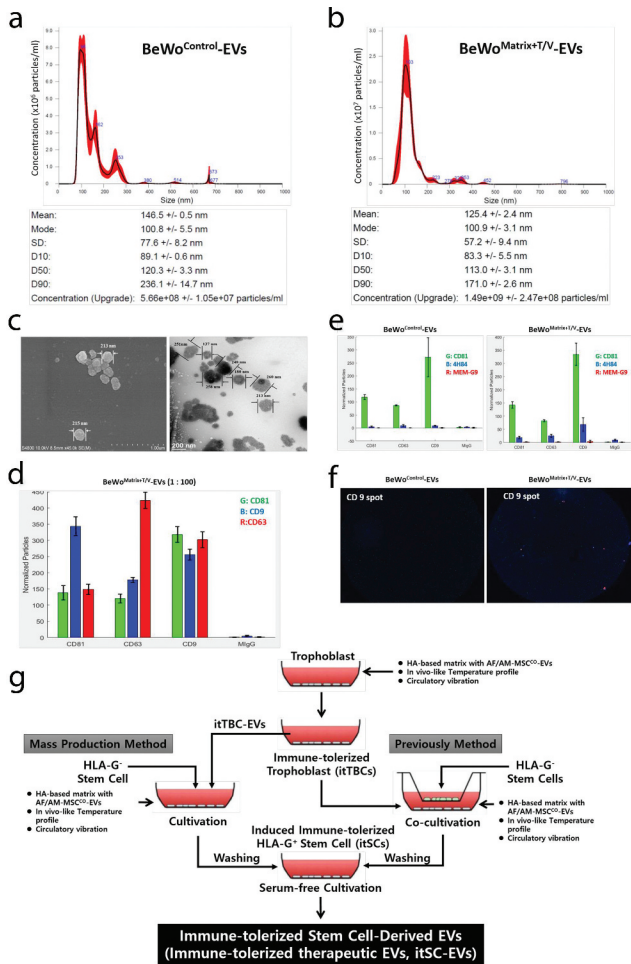
Figure 4. Characterization and Evaluation of itTBC-EVs and a scheme for induction of immune-tolerized stem cells (itSCs) and immune-tolerized EVs (itSC-EVs) through cultivation on HA-Matrix^Decidua^ containing itTBC-EVs with temperature/vibration conditions. (a) NTA analysis of EVs derived from BeWo^Control^ cultured on a general culture plate without temperature/vibration conditions. (b) NTA analysis of EVs derived from BeWo^Matrix+T/V^ cultured on the HA-Matrix^Decidua^ with the in vivo-like temperature change and vibration conditions. BeWo^Matrix+T/V^-EVs have more EV particles than BeWo^Control^ due to high proliferation rate during invasion to the HA-Matrix^Decidua^. (c) The images of BeWo^Matrix+T/V^-EVs using SEM (left) and TEM (right), respectively. (d)The expression of exosomal markers, CD9, CD63, and CD81, on BeWo^Matrix+T/V^-EVs using ExoView. (e) The expression of HLA-G isoforms in BeWo^Matrix+T/V^-EVs and BeWo^Control^-EVs using ExoView. The expressions of 4H84, bound to α1 domain of HLA-G heavy chain (with blue bar), and MEM-G/9, bound to β2 m-associated HLA-G isoforms (with red bar) are much higher in BeWo^Matrix+T/V^-EVs than BeWo^Control^-EVs. (F) The images of HLA-G-bound EV spots (blue and red) captured with CD9 antibody using ExoView. (g) A diagram for two methods to induce immune-tolerized stem cells (itSCs) and immune-tolerized EVs (itSC-EVs), by co-cultivation with itTBCs (right) and by using itTBC-EVs (left) under the Ex-vivo culture system established herein.

Characterization and evaluation of HLA-G expression and secretion of immune-tolerized stem cells (itSCs) on HA-matrix containing itTBC-EVs with in vivo-like temperature profile and circulation conditions

We designed a new ex-vivo culture system using the HA-Matrix^Decidua+itTBC-EVs^, which contains itTBC-EVs in the HA-Matrix^Decidua^ established before. And we applied this system to the MSCs (HLA-G^Negative^-

MSCs) that do not express HLA-G to confirm whether the immune-tolerance characteristic to express and secrete a variety of HLA-G isoforms, such as itTBCs established above, can be induced. To prepare an in vitro matrix optimized for the proliferation characteristics of MSCs, quite different from trophoblast cells, we performed cell proliferation assay for the culture medium containing various concentrations of itTBC-EVs after seeding hMSCs in HA-Matrix prepared by adding various concentrations of HA. As a result, HA-Matrix$^{Decidua+itTBC-EVs}$ was developed by determining the optimal HA and itTBC-EVs concentrations showing the highest hMSC proliferation and recovery (data not shown).

Figure 5(a) is a schematic diagram demonstrating that HLA-G^{Negative}-MSCs cultured in HA-Matrix$^{Decidua+itTBC-EVs}$ are the immune-tolerized stem cells (itSCs) that secrete and express various HLA-G isoforms like itTBCs. HLA-G^{Negative}-MSCs were seeded and cultured on HA-Matrix$^{Decidua+itTBC-EVs}$ under the same temperature and vibration conditions as the culture of itTBCs. Cell proliferation assay was performed while the subculture progressed. As a result, as in the case of itTBCs, the proliferation rate of MSCs (MSC$^{Matrix+T/V}$) cultured under the ex-vivo culture system reflecting the temperature change and vibration conditions in HA-Matrix$^{Decidua+itTBC-EVs}$ were quite higher than that of MSC^{Control} cultured on a general culture plate as the culture progressed (Figure 5(b)). Also, we performed PCR analysis for the intracellular HLA-G mRNA expression of MSCs using the HLA-G primer set previously used to identify various HLA-G mRNA isoforms expression in MSC$^{Matrix+T/V}$. It was confirmed that all HLA-G mRNA isoforms (HLA-G1, G2, G5, and G6) were expressed in the lysate of MSC$^{Matrix+T/V}$ (Figure 5(c)). Then, flow cytometry was performed on surface markers expressed in each MSCs. As a result of comparing the expression of representative MSC surface markers, the expression patterns of CD90 and CD105 expressed on the surface of MSC$^{Matrix+T/V}$ and MSC^{Control} showed no significant difference (Figure 5(d)). However, flow cytometry using the MEM-G/9 HLA-G antibody revealed that almost all MSC$^{Matrix+T/V}$ cells expressed membrane HLA-G, while only 12.6% of MSC^{Control} express membrane HLA-G (Figure 5(e)). Moreover, the sHLA-G concentration was measured by ELISA in the EV-enriched solutions obtained from the culture supernatant of each MSCs (Figure 5(f)). The result showed that the level of the sHLA-G in the EVs from in the culture supernatant of MSC$^{Matrix+T/V}$ was much higher than that of MSC^{Control}. In particular, it was also confirmed that soluble HLA-G5/6 in the EVs derived from MSC$^{Matrix+T/V}$ were contained much more than in the EVs derived from MSC^{Control}, which mean that the sHLA-G in the EV-enriched solution

from MSC^{Control} was almost membrane bound HLA-G1 shedded from the cell surface, not HLA-G5/6 secreted from MSCs, but sHLA-G in the EV-enriched solution from MSC$^{Matrix+T/V}$ included considerable amount of HLA-G5/6 secreted from MSCs. These results are consistent with the previous study [26], which demonstrates that soluble HLA-G present in the supernatant of MSC is not HLA-G5 secreted from MSC, but HLA-G1 shedded from the cell membrane.

From these results, we demonstrated that HLA-G^{Negative}-MSCs cultured on HA-Matrix$^{Decidua+itTBC-EVs}$ with the in vivo-like temperature change and vibration conditions could be induced to the immune-tolerized stem cells (itSCs) that continuously secrete and express various HLA-G isoforms like itTBCs. Besides, the itTBC-EVs added in the HA-Matrix$^{Decidua+itTBC-EVs}$ increase the secretion of soluble HLA-G, which is due to the transcription of the EVT-specific characteristic to secrete soluble HLA-G at the mother-foetal interface continuously. However, as a result of analysing the relative intensity of 1,358 proteins contained in each EVs obtained through the serum-free culture of MSC^{Control} and itSCs through Signalling Explorer Antibody Array, the overall protein secretion level was slightly higher in itSCs, which showed better cell proliferation rate than MSC^{Control}. But, there is no significant difference in secretory profile (Figure 5(g)). This finding indicates that MSCs cultured in the ex-vivo culture system are newly transcribed only immune tolerance properties capable of expressing and secreting various HLA-G isoforms while maintaining their unique MSC properties.

Characterization of EVs (itSC-EVs) from cultivation of immune-tolerized stem cells (itSCs) on the HA-Matrix$^{Decidua+itTBC-EVs}$ with in vivo-like temperature profile and circulation conditions

Culture supernatant of itSCs were centrifuged at low speed to remove cell debris, then itSC-EVs were collected by multi-stage filtration. Their size and concentration were determined and compared with EVs from MSC^{Control} by NTA (n = 3). The concentrations of MSC^{Control}-EVs varied between individual preparations ranging from $1.14 \times 10^9 \pm 2.78 \times 10^7$ particles/ml obtained from 1.0×10^5 MSC^{Control} approximately (Figure 6(a)), and that of MSC$^{Matrix+T/V}$ were $1.42 \times 10^9 \pm 2.47 \times 10^8$ particles/ml obtained from 1.0×10^5 MSC$^{Matrix+T/V}$ approximately, rather higher than MSC^{Control}-EVs (Figure 6(b)). The MSC-EVs size distribution profiles of each 3 samples were similar each other. But, MSC^{Control}-EVs between 50 and 300 nm were detected, while MSC$^{Matrix+T/V}$-EVs between 50 and 500 nm were detected. The average
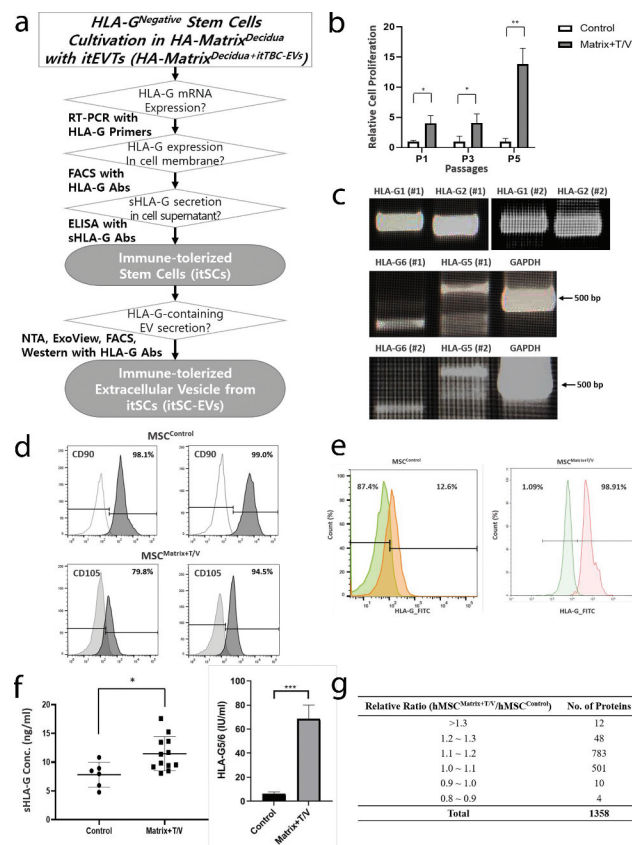
Figure 5. Proliferation and evaluation of HLA-G expression and secretion of cultured MSCs on the HA-Matrix^Decidua+itTBC-EVs containing itTBC-EVs with in vivo-like temperature change and circulation conditions. (a) A scheme of verification procedure for induction of immune-tolerized stem cells (itSCs) and immune-tolerized EVs (itSC-EVs) secreted from itSCs. (b) Relative cell proliferation assay of HLA-G^Negative-MSCs cultured on the 2D-culture plate (Control) and on the HA-Matrix^Decidua+itTBC-EVs under temperature/vibration conditions (Matrix+T/V). The proliferation rate of MSC^Matrix+T/V was much higher than MSC^Control. Error bars represent SD. *, P < 0.05; **, P < 0.01; t-test; (c) Intracellular HLA-G mRNA isoforms expression of MSCs obtained at passage 5 from cultivation on the HA-Matrix^Decidua+itTBC-EVs under temperature/vibration conditions (MSC^Matrix+T/V) was shown by RT-PCR analysis, with GAPDH as a positive control, using designed HLA-G primer set listed in Supplemental Table. 1. All HLA-G mRNA isoforms (HLA-G1, G2, G5, and G6) were expressed. (d) FACS analysis of MSC markers (CD90 and CD105) on the surface of the MSC^Matrix+T/V and MSC^Control obtained at passage 5. (e) FACS analysis of membrane-bound HLA-G expression on the surface of MSC^Control and MSC^Matrix+T/V obtained at passage 5 using MEM-G/9 antibody. The result shows that a much higher proportion of MSC^Matrix+T/V expresses membrane HLA-G than MSC^Control. (f) The concentrations of sHLA-G (left) and HLA-G5/6 (right) in the EV-enriched solution of MSC^Matrix+T/V and MSC^Control obtained at passage 5 using MEM-G/9 and 5A6G7 Abs, respectively. The level of sHLA-G, especially HLA-G5/6 secreted from MSCs, is much higher in MSC^Matrix+T/V than MSC^Control. Error bars represent SD. *, P < 0.05; ***, P < 0.001; Mann Whitney test. (G) Comparison of protein secretion profiles of EV-enriched solution secreted from MSC^Matrix+T/V and MSC^Control obtained at passage 5 using Signalling Explorer Antibody Array. Total 1,358 kinds of human protein were detected in both EV-enriched solutions with similar intensities.

modal size and the average mean size of MSC^Control-EVs were 96.0 ± 5.6 nm and 138.0 ± 2.2 nm, respectively. While, the average modal size and the average mean size of MSC^Matrix+T/V-EVs were 128.7 ± 5.0 nm and 152.5 ± 1.4 nm, respectively, rather bigger than MSC^Control-EVs. The concentration of total proteins of MSC^Matrix+T/V-EVs was 597.24 ± 18.25 μg/ml through BCA protein assay, rather higher than MSC^Control-EVs (457.64 ± 21.63 μg/ml).

Figure 6(c) shows the images of MSC^Matrix+T/V-EVs with a scanning electron microscope (SEM) and a transmission electron microscope (TEM), respectively. Figure 6(d) shows that MSC^Matrix+T/V-EVs was positive for exosomal markers of CD9, CD63 and CD81 by flow cytometry. Also, co-expression of exosomal markers and HLA-G antibody was analysed by flow cytometry. The upper panel of Figure 6(e) represents a FACS analysis of reference-size beads used to gate the proper areas to examine the expected-size EVs. The lower panel of Figure 6(e) shows that most of the EVs detected in the gating area are double-positive EVs for HLA-G/CD9 and HLA-G/CD63, respectively (Figure 6(e)). ExoView conducted each MSC-derived EVs analysis. As a result, it was confirmed that the 4H84 antibody that specifically binds
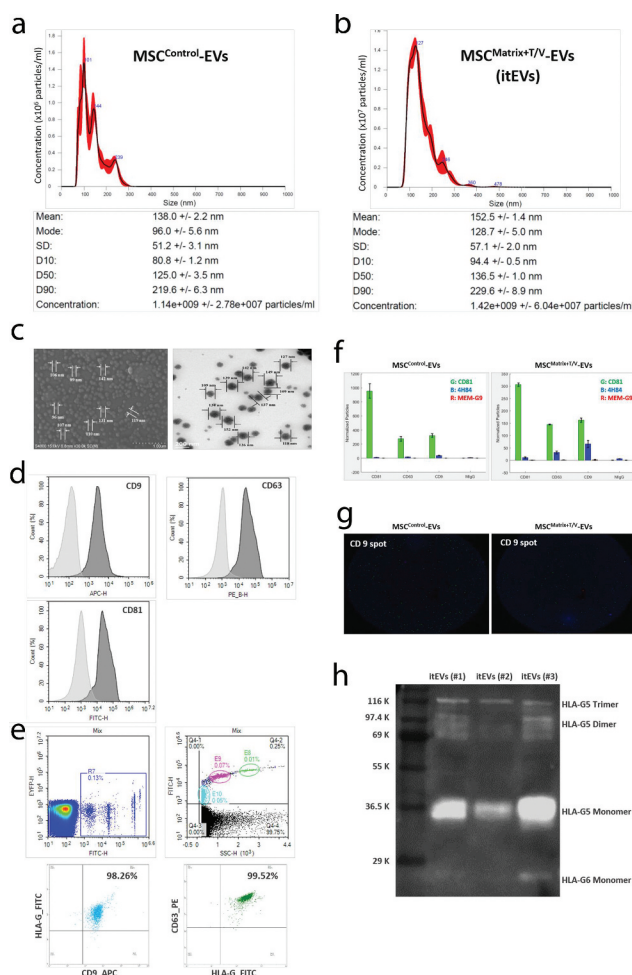
Figure 6. Characterization and Evaluation of itSC-EVs. (a) NTA analysis of EVs derived from MSC^{Control} cultured on a general culture plate without temperature/vibration conditions. (b) NTA analysis of EVs derived from MSC$^{Matrix+T/V}$ cultured on the HA-Matrix$^{Decidua +itEVT}$ containing itTBC-EVs with the in vivo-like temperature change and vibration conditions. MSC$^{Matrix+T/V}$-EVs (itSC-EVs) have more EV particles than MSC^{Control} due to high proliferation rate in the ex-vivo culture system. (c) The images of MSC$^{Matrix+T/V}$-EVs using SEM (left) and TEM (right), respectively. (d) FACS analysis of MSC$^{Matrix+T/V}$-EVs to investigate the expression of exosomal markers (CD9, CD63 and CD81) (E) FACS analysis of MSC$^{Matrix+T/V}$-EVs to investigate the co-expression of exosomal markers (CD9 and CD63) and HLA-G (MEM-G/9). The upper panel represents analysis of reference beads with different sizes. The light blue-coloured area is gating for 100 nm-size beads, the pink-coloured area is gating for 200 nm-size beads, and the green-coloured area is gating for 500 nm-size beads, respectively. The lower panel shows FACS analysis of double-stained MSC$^{Matrix+T/V}$-EVs, HLA-G/CD9 (left) and HLA-G/CD63 (right). (f) The expression of HLA-G isoforms in MSC$^{Matrix+T/V}$-EVs and MSC^{Control}-EVs using ExoView. The expressions of 4H84 (with blue bar) is much higher in MSC$^{Matrix+T/V}$-EVs than MSC^{Control}-EVs. (g) The capture images of HLA-G-bound EV spots (blue and red) captured with CD9 antibody using ExoView. (h) Western blot analysis of MSC$^{Matrix+T/V}$-EVs for soluble HLA-G5/G6 detection using 5A6G7 antibody. Three individually prepared MSC$^{Matrix+T/V}$-EVs contains HLA-G5 monomer, dimer and trimer forms, and HLA-G6 monomer in a MSC$^{Matrix+T/V}$-EVs. These findings show that MSC$^{Matrix+T/V}$-EVs is the immune-tolerized EVs (itEVs) containing various HLA-G isoforms. Error bars represent SD.

to the α1 domain of all HLA-G heavy chain was much higher in MSC$^{Matrix+T/V}$-EVs than MSC^{Control} (Figure 6 (f)). Comparing EV spots captured with CD9 antibody among exosome markers, it was also confirmed that more EV spots coupled with HLA-G antibodies (blue) were present in MSC$^{Matrix+T/V}$-EVs (Figure 6(g)). Finally, to detect soluble HLA-G protein contained in MSC$^{Matrix+T/V}$-EVs, western blot analysis was performed using the 5A6G7 antibody that specifically binds only to intron 4 of soluble HLA-G5 and G6. HLA-G5 monomers, dimers

and trimers were detected in three MSC$^{Matrix+T/V}$-EVs prepared independently, and HLA-G6 monomers were detected in one MSC$^{Matrix+T/V}$-EVs (Figure 6(h)). The expression level of the HLA-G6 dimer was so weak that it could not be accurately identified. But it was also recognized at the position estimated by HLA-G5-G6 trimer, suggesting that HLA-G6 dimer is also present.

From these findings, we confirmed that the EVs secreted from MSCs cultured in HA-Matrix$^{Decidua+itTBC-EVs}$ expresses membrane-bound HLA-G and contains both

soluble HLA-G5 and G6. Namely, we have demonstrated all of the hypotheses we have established by reproducing the induction of immune-tolerized stem cell lines (itSCs) and obtaining immune-tolerized EVs (itSC-EVs) from in vitro culture conditions established herein.

The potential for induction of immune tolerance by itSC-EVs

To evaluate the immune tolerance inductive potential of itSC-EVs, we compared their effect on T-cell proliferation and T_{reg}-cell differentiation with $MSC^{Control}$-EVs, because MSCs and their EVs were known to have immunomodulatory potential. CFSE pre-labelled PBMCs were stimulated with PHA and co-cultured with $MSC^{Control}$-EVs and $MSC^{Matrix-T/V}$-EVs for five days, respectively. $MSC^{Control}$-EVs and $MSC^{Matrix-T/V}$-EVs were obtained from serum-free cultivation of the same number of $MSC^{Control}$ and $MSC^{Matrix-T/V}$ as stimulated PBMCs. As shown in Figure 7(a), the proliferation of $CD3^+$ T-cell was significantly inhibited by $MSC^{Matrix+T/V}$-EVs treatment on PHA-stimulated PBMCs compared with $MSC^{Control}$-EVs. In addition, the differentiation of $CD3^+$ T-cell to T_{reg}-cell was dramatically induced by $MSC^{Matrix+T/V}$-EVs treatment on PHA-stimulated PBMCs compared with $MSC^{Control}$-EVs.

From these results, we demonstrated that $MSC^{Matrix+T/V}$-EVs (itSC-EVs) have the remarkable capacity to reduce T cell proliferation (induce local immune tolerance by both membrane-bound HLA-G and soluble HLA-G isoforms) and to promote T_{reg} cell differentiation (induce extensive immune tolerance by soluble HLA-G isoforms).

Discussion

Immunogenicity has emerged as a significant problem with allogeneic and autologous stem cell transplantation, and many strategies available for controlling such unwanted responses were under development [27]. In pursuit of developing cell- or EV-based therapeutics without these immune responses, we noted on the pregnancy phenomenon where immune rejection is naturally inhibited. Namely, the immune tolerant environment where a semi-allogeneic foetus is entirely protected by HLA-G as a natural immunosuppressant from the maternal immune system was the solution. To explain this, we established several hypotheses of *in vivo* environmental factors that induce immune tolerance by EVT-specific HLA-G at the maternal-foetus interface. And, we designed the ex-vivo culture system (HA-Matrix^{Decidua}) simulating them, where we
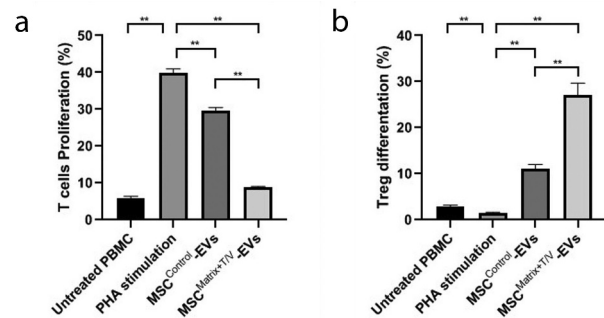
Figure 7. T-cell Proliferation Assay and T_{reg}-cell differentiation Assay of $MSC^{Control}$-EVs and $MSC^{Matrix+T/V}$-EVs (itSC-EVs). CFSE pre-labelled PBMCs were stimulated with 5 µg/ml of PHA and co-cultured with $MSC^{Control}$-EVs and $MSC^{Matrix+T/V}$-EVs for 5 days, respectively. Each EVs were obtained from the same number of MSCs with PBMCs. (a) $MSC^{Matrix+T/V}$-EVs are much more effective to inhibit the proliferation of $CD3^+$ T-cell than $MSC^{Control}$-EVs on PHA-stimulated PBMCs. (b) $MSC^{Matrix+T/V}$-EVs have a remarkable effect on the induction of $CD3^+/CD25^+$ T_{reg}-cell differentiation from total $CD3^+$ T-cell compared with $MSC^{Control}$-EVs. Error bars represent SD. **, P < 0.01; the Student's t-test.

cultured trophoblast cells and stem cells with very low HLA-G expression. As a result, we demonstrated to induce the immune-tolerized cell lines (itTBCs and itSCs) like EVTs during pregnancy that continued to express membrane-bound HLA-G1/2 and secrete soluble HLA-G5/6 proteins. Especially, itSCs can maintain their immune-tolerant characteristics secreting various HLA-G isoforms and HLA-G-containing EVs in general cultivating conditions without HA-Matrix^{Decidua}. This finding should shed light on application for allograft cell- or EV-based therapeutics having increased survival duration by not causing immune-rejection, as demonstrated in the previous study [28]; therefore, superior curative effects can be expected.

Figure 8(a) shows the verification of hypotheses of in vivo environmental factors stimulating EVT-specific HLA-G expression and secretion, as suggested in Supplemental Figure 1A. Although the subsequent studies could be needed for more detailed investigations, we would like to explain the immune tolerance mechanism induced during pregnancy through our experimental results as follows: (i) mechanisms for HLA-G transcription and alternative splicing causing formation of soluble HLA-G isoforms stimulated by pregnancy-related hormone; (ii) mechanism for expression and secretion of various HLA-G isoforms as like EVTs in the decidua; (iii) mechanism for formation of HLA-G homodimer having superior immune tolerance features than monomer; and (iv) mechanism for overall immune tolerance by various HLA-G isoforms and HLA-G-containing EVs.
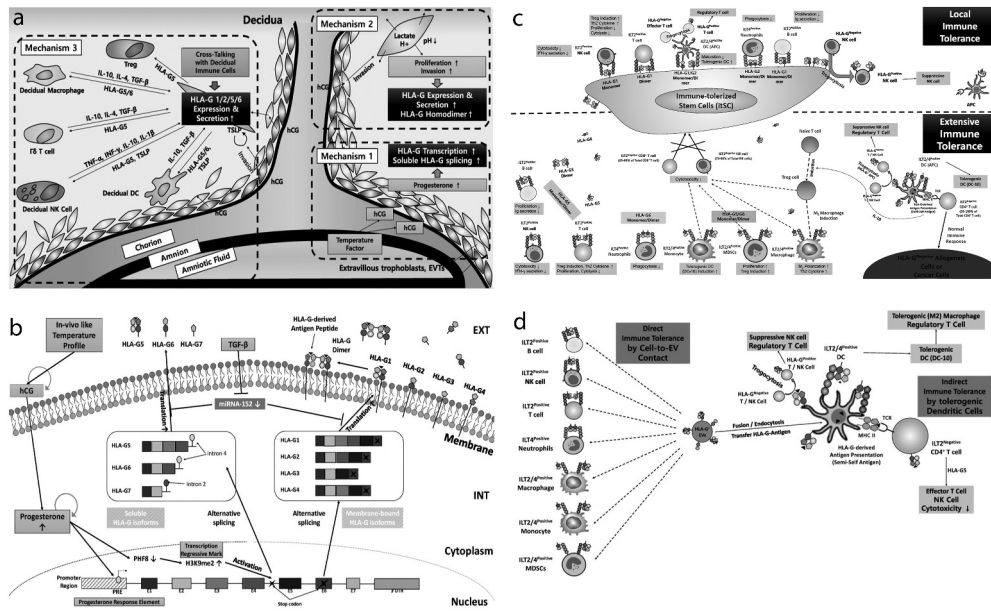
Figure 8. Proposed mechanisms for pregnancy-related hormone-dependent HLA-G gene transcription and alternative splicing in immune-tolerized trophoblast cells (itTBCs) and induction of immune-tolerance environment by HLA-G isoforms and HLA-G-containing EVs. (a) The entire immune tolerance mechanism during pregnancy. "Mechanism 1" shows upregulated HLA-G gene transcription and alternative splicing to form soluble HLA-G mRNA isoforms stimulated by progesterone. "Mechanism 2" reveals the elevated HLA-G expression and secretion of EVTs during invasion and proliferation at the decidua stimulated by hCG. It also shows the increased formation of HLA-G homodimer. "Mechanism 3" demonstrates the expression and secretion of various HLA-G isoforms through the cross-talking between decidual immune cells and EVTs in the foetal membrane structure. (B) The overall mechanism for HLA-G transcription, alternative splicing, the formation of various isoforms, expression of membrane-bound HLA-G, and secretion of soluble HLA-G in EVTs and itTBCs. (c) The upper part shows the local immune tolerance mechanism by membrane-bound HLA-G isoforms binding with inhibitory receptors of various immune cells, including NK, T, B cell, DCs, and neutrophils. The lower part reveals the extensive immune tolerance mechanism due to soluble HLA-G isoforms by binding with the receptors of immune cells and transfer of HLA-G-derived antigen to APCs. (d) Immune tolerance mechanisms by HLA-G-containing EVs. Direct immune tolerance is established by contact of EVs to immune cells. Indirect immune tolerance is induced by differentiation into tolerogenic immune cells (DC-10, Treg, and M2 macrophage) and by HLA-G-derived antigen presentation to APCs and CD4^{+} T cells.

Progesterone, induced by in-vivo like temperature change, may act as the initiator of HLA-G transcription as well as the mediator of alternative splicing for soluble HLA-G isoforms

Because soluble HLA-G5/6 can induce more extensive immune tolerance in comparison to local immune tolerance by membrane-bound HLA-G1/2, the fact that EVTs can secrete both soluble HLA-G5/6 should be the prerequisite for maintaining a healthy pregnancy. However, unlike other HLA Class I molecules incapable of producing soluble isoforms, it is still unknown why a premature stop codon, located in intron 4 of the HLA-G gene, is matured in EVTs only leading to create soluble HLA-G isoforms. According to the recent study [29], depletion of PHF 8 (Plant Homeodomain Finger protein 8), a histone demethylase of H3K9 (lysine residue 9 on histone H3), in HUVECs (Human umbilical vein endothelial cells)

and JEG3 cells, led to increased H3K9me2 (dimethylated state of H3K9) levels within intron 4 of the HLA-G gene. Consequently, the stop codon located in intron 4 of the HLA-G gene is matured to terminate the transcription process, increasing the expression of soluble HLA-G5/6 mRNAs containing intron 4. We verified the hypotheses that progesterone, induced by in vivo-like temperature change starting-up hormone expression in replacement of the nervous system, can stimulate HLA-G transcription in itTBCs and itSCs by demonstrating that they could secrete soluble HLA-G5/6. There is no study about the relation between PHF 8 and pregnancy related hormones. However, our findings may support a new mechanism that progesterone, upregulated in our ex-vivo culture system, gets involved in alternative splicing of the HLA-G gene to stimulate the formation of soluble HLA-G5/6 mRNA isoforms critical to the establishment of extensive immune tolerance environment (Figure 8(b)).

TGF-β enriched in HA-Matrix^Decidua may enhance the post-transcriptional stability of HLA-G mRNA via downregulating miRNA targeting HLA-G

The expression levels of miR-148 and miR-152, known as HLA-G-targeting miRNAs, are downregulated in the placenta compared with other healthy tissues [30], but the reason is still unknown. Merely, we can assume that the decrease in the level of these miRNAs in trophoblast cells is necessary for proper implantation and pregnancy maintenance from the finding that overexpression of miR-152 reduced HLA-G mRNA level in trophoblast cells and the placenta during preeclampsia [31]. To investigate the cause, we compared Quantibody Human Cytokine Array 1000 results (Figure 2(d)) with the concentration of soluble HLA-G5/6 in itTBC-EVs obtained from each experiment, respectively. The exciting results show that the higher the level of TGF-β, present in a relatively higher amount amongst other proteins in AF/AM-MSC^CO-EVs, the higher the concentration of soluble HLA-G5/6 in itTBC-EVs (data not shown). From this finding, we can assume that TGF-β may relate to the expression of HLA-G-targeting miRNAs. Referring to the recent study [32] that TGF-β inhibited the expression of miR-152 in colorectal cancer cells, we can explain that TGF-β downregulates miR-152 of itTBCs and itSCs and thereby, leads to the increases of the expression and secretion of HLA-G (Figure 8(b)).

Soluble factors from decidual immune cells induce various HLA-G isoforms and form a positive loop to sustain spontaneous HLA-G secretion in EVTs

At the maternal-foetal interface, EVTs secrete Thymic Stromal Lymphopoietin (TSLP), stimulated by Interleukin (IL)-10, IL-1β, INF-γ, and Tumour Necrosis Factor (TNF)-α secreted from decidual NK cells (dNK) and progesterone from STBs. TSLP stimulates EVTs proliferation, invasion, and HLA-G secretion in an autocrine manner, then induces secretion of IL-10 and TGF-β in decidual Dendritic Cells (dDCs) and γδ-T cells. These cytokines induce differentiation of regulatory T cells (T_reg) and decidual macrophages (dMΦ) having immune-tolerant characteristics and further increase HLA-G secretion in EVTs. This HLA-G repeatedly induces secretion of Th2 cytokines (IL-10, TGF-β) in dMΦ. As a result, a circuit may exist continuously stimulating HLA-G secretion of EVTs inducing an extensive immune tolerance environment. We established a positive loop, as shown in Figure 8(a), maintaining spontaneous HLA-G expression and secretion of EVTs by various immunosuppressive soluble factors (i.e., IL-1β, IL-10, TGF-β, IFN-γ and TNF-

α) from decidual immune cells, which already existed in AF/AM-MSC^CO-EVs, as shown in Figure 2(d,e).

β2m-free HLA-G2 and G6, together with β2m-associated HLA-G1 and G5, may play a key role in building a local- and extensive-immune tolerance environment

Immune tolerance by HLA-G is mainly due to binding with target immune cells' various receptors, including Ig-Like Transcript 2 (ILT2), ILT4, CD8, CD160 and Killer cell Immunoglobulin-like receptor 2DL4 (KIR2DL4). ILT2 exists on all monocytes and B cells, some DCs, Myeloid-derived suppressor cells (MDSCs), NK, and T cells, binding with α3 domain and β2m of MHC I molecules [33]. ILT4 is an inhibitory receptor expressed almost exclusively in myeloid monocyte lineage cells, such as monocytes, dendritic cells, neutrophils, and MDSCs [34,35]. These receptors preferentially bind to the HLA-G α3 domain, which has a unique sequence compared to other MHC I molecules [36]. They have a higher binding affinity for dimers than monomers [37]. ILT2 can recognize β2m-associated HLA-G1/G5 only, but ILT4 can bind β2m-free HLA-G2/G6 as well as β2m-associated HLA-G [35,36]. For further studies on immune tolerance by HLA-G binding to inhibitory receptors of individual immune cells, refer to the review [38].

From our result, we aim to explain the overall mechanism of immune tolerance during pregnancy built by various HLA-G isoforms and HLA-G-containing EVs anew.

Firstly, it is the local immune tolerance mechanism by direct contacts between membrane-bound HLA-G1/2, present in the immune-tolerized cells or EVs surface, and immune cells. As shown in the upper panel of Figure 8(c), HLA-G^Positive cells binding ILT inhibitory receptors of immune cells reduce their activities variously. However, unlike immune cells in decidua during pregnancy, among peripheral blood immune cells, only 0 ~ 5% of CD4^+ T cells, 10 ~ 15% of CD8^+T cells, and 20 ~ 25% of NK cells are known to express HLA-G-bonding ILT2 inhibitors [33]. This finding shows that the local immune tolerance through cell-to-cell contact would not be effective against most of the immune cells not expressing ILT2.

Secondly, we assumed that soluble HLA-G5/G6-induced the extensive immune tolerance mechanism would be critical to induce immune-tolerance during pregnancy. As shown in the lower part of Figure 8(c), soluble HLA-G5/6, secreted by itTBCs and itSCs, can establish a much broader extensive immune tolerance

environment than local immune tolerance through membrane-bound HLA-G1/2 contact. The Immune tolerance mechanism by binding between ILT2/4 receptors of immune cells with soluble HLA-G5/6 is similar to local immune tolerance. But, in respect of establishing the entire immune tolerance environment including immune cells with no HLA-G-binding receptors, we noted that tolerogenic DCs (DC-10), induced by binding with HLA-G5/6, will play a critical role as the followings:

(i) DC-10 exhibit tolerogenic characteristics with overexpression of HLA-G and especially ILT-4 on their surface. And they inhibit immune reaction by trogocytosis through contacts with the majority of NK and T cells lacking HLA-G-binding inhibitory receptors. From the fact of ILT4 overexpression on APCs [39], we propose a new mechanism that β2m-free HLA-G6, having a higher binding affinity than β2m-associated HLA-G5 to ILT4 receptor, can play a critical role in inducing DC-10. The fact that only EVTs, present at the maternal-foetal interface, secrete HLA-G6 supports this.

(ii) Immunosuppressive cytokines, such as IL-10 and TGF-ß, secreted by DC-10 induce differentiation of T_{reg} cells and tolerogenic macrophage (M2 phenotype) within extensive ranges. They also secrete immunosuppressive cytokines to inhibit the cytotoxicity of NK and effector $CD8^+$T cells, resulting in a broad immune tolerance environment.

(iii) Antigen peptide, transferred by HLA-G5 secreted by itTBCs or itSCs, is processed by the APCs (professional antigen-presenting cells) like DCs and delivered to $CD4^+$ T cells through TCR. In this process, $CD4^+$ T cells, having received HLA-G5-derived antigen from APCs, along with DCs binding with HLA-G, also secret HLA-G5, thus further contributing to extensive immune tolerance environment. We want to explain this phenomenon to the new mechanism that APCs, binding with HLA-G5, may process and present HLA-G5-derived antigens to be recognized as commensal antigens or semi-self-antigens as beneficial enteric bacteria that are alive in our intestine without the immune response. However, $CD4^+$ T cells, even educated to HLA-G5-derived antigens through APCs, perform the proper immune responses against cancer cells and infected cells expressing abnormal antigens, just as mother's immune cells during pregnancy cause immune tolerance for EVTs secreting HLA-G but not against foreign viruses or pathogens.

Finally, we suggest a new immune tolerance mechanism by HLA-G-containing EVs, as shown in Figure 8(d). HLA-G-containing EVs arise not only local immune tolerance through contacts with all immune cells having HLA-G-binding receptors but also fast immune tolerance by trogocytosis through fusion with or endocytosis by APCs. Moreover, in this process, they transfer HLA-G-derived antigens to DCs to induce DC-10 causing extensive immune tolerance environment, along with antigen-educated $CD4^+$ T cells from DC-10, reducing the cytotoxicities of NK and effector $CD8^+$ T cells.

Therefore, we can say that itTBCs and itSCs are the noble cell lines with excellent immune tolerant capabilities inducing 1) local immune tolerance by contact of membrane-bound HLA-G1/G2 with immune cells or by trogocytosis, 2) extensive immune tolerance through soluble HLA-G5/G6, and 3) immune tolerance induced by HLA-G-containing EVs.

Immune-tolerized stem cells (itSCs) build the bridgehead towards the new treatment paradigm with HLA-G-containing immune-tolerized extracellular vesicles (itSC-EVs)

For easement of graft versus host reaction, the research result [4] that bone-marrow (BM)-MSC-derived exosomes containing HLA-G was useful has drawn much attention about the clinical application of HLA-G-containing EVs [40]. To date, as a source of HLA-G-containing EVs, a fraction of cancer cells, including melanoma, trophoblast during pregnancy, and BM-MSCs, are known [41]. But in HLA-G-containing EVs fraction, first discovered in cancer patients, it was found to contain ubiquitinated HLA-G proteins with the abnormal molecular size ranging from 50 to 75kD [42]. This finding is due to the abnormally repeated process of transcription-translation-degradation. As a result, these mis-synthesized proteins different from normal HLA-G suggest that proper binding characteristics to immune cells should be diminished [43].

On the other hand, we confirmed that itTBCs and itSCs express membrane-bound HLA-G1/G2 and secrete HLA-G-containing EVs and soluble HLA-G5/G6 as homodimer forms having a much higher binding affinity to inhibitory receptors of immune cells. Therefore, itSC-EVs established herein can be expected as an excellent immunosuppressant and autoimmune therapeutics, as demonstrated in Figure 7. Also, using itSC-EVs containing various biologically active substances might open up a new era of EV-based therapeutics, especially for neurodegenerative diseases, because they can pass through the blood-brain-barrier (BBB) but cell-based therapeutics can't.

Conclusions

In conclusion, we established the ex-vivo culture system simulating the maternal-foetal interface during pregnancy, demonstrated to induce immune-tolerized cell lines and EVs, and revealed the entire immune tolerance mechanism. Our findings might provide new ways to develop immune-rejection-free therapeutics using immune-tolerized cells and EVs.

Author Contributions

Jangho Lee conceived the idea, established all hypotheses and supported the funding.
Jangho Lee and Kyoungshik Cho conceived and designed all experiments and drafted and revised the manuscript.
Kyoungshik Cho, Hyejin Kook, and Suman Kang performed and analysed most of the experiments.

Disclosure statement

The authors declare no competing financial interest.

ORCID

Kyoungshik Cho (ID) http://orcid.org/0000-0001-5085-5574
Hyejin Kook (ID) http://orcid.org/0000-0001-7667-4640
Suman Kang (ID) http://orcid.org/0000-0001-9621-9215
Jangho Lee (ID) http://orcid.org/0000-0003-0772-9438

References

[1] Tetta C, Ghigo E, Silengo L, et al. Extracellular vesicles as an emerging mechanism of cell-to-cell communication. Endocrine. 2013;44:11–19.

[2] Arslan F, Lai RC, Smeets MB, et al. Mesenchymal stem cell-derived exosomes increase ATP levels, decrease oxidative stress and activate PI3K/Akt pathway to enhance myocardial viability and prevent adverse remodeling after myocardial ischemia/reperfusion injury. Stem Cell Res. 2013;10:301–312.

[3] Gallina C, Turinetto V, Giachino C. A new paradigm in cardiac regeneration: the mesenchymal stem cell secretome. Stem Cells Int. 2015;2015:765846.

[4] Kordelas L, Rebmann V, Ludwig AK, et al. MSC-derived exosomes: A novel tool to treat therapy-refractory graft-versus-host disease. Leukemia. 2014;28:970–973.

[5] Bruno S, Grange C, Collino F, et al. Microvesicles derived from mesenchymal stem cells enhance survival in a lethal model of acute kidney injury. PLoS One. 2012;7:e33115.

[6] Tan CY, Lai RC, Wong W, et al. Mesenchymal stem cell-derived exosomes promote hepatic regeneration in drug-induced liver injury models. Stem Cell Res Ther. 2014;5:76.

[7] Xin H, Li Y, Buller B, et al. Exosome-mediated transfer of miR-133b from multipotent mesenchymal stromal cells to neural cells contributes to neurite outgrowth. Stem Cells. 2012;30:1556–1564.

[8] Zhang B, Yin Y, Lai RC, et al. Mesenchymal stem cells secrete immunologically active exosomes. Stem Cells Dev. 2014;23:1233–1244.

[9] Liu Q, Rojas-Canales DM, Divito SJ, et al. Donor dendritic cell-derived exosomes promote allograft-targeting immune response. J Clin Invest. 2016;126:2805–2820.

[10] Cataldi M, Vigiotti C, Mosca T, et al. Emerging role of the spleen in the pharmacokinetics of monoclonal antibodies, nanoparticles and exosome. Int J Mol Sci. 2017;18:1249.

[11] Wang D, Quan Y, Yan Q, et al. Targeted disruption of the β2-microglobulin gene minimizes the immunogenicity of human embryonic stem cells. Stem Cells Transl Med. 2015;4:1234–1245.

[12] Xu H, Wnag B, Ono M, et al. Targeted disruption of HLA genes via CRISPR-Cas9 generates iPSCs with enhanced immune compatibility. Cell Stem Cell. 2019;24:566–578.

[13] Gornalusse GG, Hirata RK, Funk S, et al. HLA-E-expressing pluripotent stem cells escape allogeneic responses and lysis by NK cells. Nat Biotechnol. 2017;35:765–772.

[14] Deuse T, Hu X, Gravina A, et al. Hypoimmunogenic derivatives of induced pluripotent stem cells evade immune rejection in fully immunocompetent allogeneic recipients. Nat Biotechnol. 2019;37:252–258.

[15] Ellis SA, Sargent IL, Redman CW, et al. Evidence for a novel HLA antigen found on human extravillous trophoblast and a choriocarcinoma cell line. Immunology. 1986;59:595–601.

[16] Carosella ED, Moreau P, Le Maoult J, et al. HLA-G molecules: from maternal-fetal tolerance to tissue acceptance. Adv Immunol. 2003;81:199–252.

[17] Gregori S, Tomasoni D, Pacciani V, et al. Differentiation of type 1 T regulatory cells (Tr1) by tolerogenic DC-10 requires the IL-10-dependent ILT4/HLA-G pathway. Blood. 2010;116:935–944.

[18] Amodio G, Mugione A, Sanchez AM, et al. HLA-G expressing DC-10 and CD4^{+} T cells accumulate in human decidua during pregnancy. Hum Immunol. 2013;74:406–411.

[19] Amodio G, Sales de Albuquerque R, Gregori S. New insights into HLA-G mediated tolerance. Tissue Antigens. 2014;84:255–263.

[20] Castelli EC, Veiga-Castelli LC, Yaghi L, et al. Transcriptional and Posttranscriptional Regulations of the HLA-G gene. J Immunol Res. 2014;2014:734068.

[21] Bax BE, Bloxam DL. Energy metabolism and glycolysis in human placental trophoblast cells during differentiation. Biochim Biophys Acta. 1997;1319:283–292.

[22] Hunt JS. Stranger in a strange land. Immunol Rev. 2006;213:36–47.

[23] Hannan NJ, Paiva P, Dimitriadis E, et al. Models for study of human embryo implantation: choice of cell lines? Biol Reprod. 2010;82:235–245.

[24] Apps R, Gardner L, Sharkey AM, et al. A homodimeric complex of HLA-G on normal trophoblast cells modulates antigen-presenting cells via LILRB1. Eur J Immunol. 2007;37:1924–1937.

[25] Gonen-Gross T, Achdout H, Gazit R, et al. Complexes of HLA-G protein on the cell surface are important for leukocyte Ig-like receptor-1 function. J Immunol. 2003;171:1343–1351.

[26] Giuliani M, Fleury M, Vernochet A, et al. Long-lasting inhibitory effects of fetal liver mesenchymal stem cells on T-lymphocyte proliferation. PLoS ONE. 2011;6:e19988.

[27] Wood KJ, Issa F, Hester J. Understanding stem cell immunogenicity in therapeutic applications. Trends Immunol. 2016;37:5–16.

[28] LeMaoult J, Daouya M, Wu J, et al. Synthetic HLA-G protein for therapeutic use in transplantation. Faseb J. 2013;27:3643–3651.

[29] Leisegang MS, Gu L, Preussner J, et al. The histone demethylase PHF8 facilitates alternative splicing of the histocompatibility antigen HLA-G. FEBS Lett. 2019;593:487–498.

[30] Manaster I, Goldman-Wohl D, Greenfield C, et al. MiRNA-mediated control of HLA-G expression and function. PLoS ONE. 2012;7:e33395.

[31] Vashukova ES, Glotov AS, Baranov VS. MicroRNAs associated with preeclampsia. Russian J Genetics. 2020;56:1–16.

[32] Guan Z, Song B, Liu F, et al. TGF-β induces HLA-G expression through inhibiting miR-152 in gastric cancer cells. J Biomed Sci. 2015;22:107.

[33] Rouas-Freiss N, Moreau P, LeMaoult J, et al. The dual role of HLA-G in cancer. J Immunol Res. 2014;2014:359748.

[34] Colonna M, Navarro F, Bellon T, et al. A common inhibitory receptor for major histocompatibility complex class I molecules on human lymphoid and myelomonocytic cells. J Exp Med. 1997;186:1809–1818.

[35] Colonna M, Samaridis J, Cella M, et al. Human myelomonocytic cells express an inhibitory receptor for classical and nonclassical MHC class I molecules. J Immunol. 1998;160:3096–3100.

[36] Ho Wang Yin KY, Loustau M, Wu J, et al. Multimeric structures of HLA-G isoforms function through differential binding to LILRB receptors. Cell Mole Life Sci. 2012;69:4041–4049.

[37] Shiroishi M, Kuroki K, Ose T, et al. Efficient leukocyte Ig-like receptor signaling and crystal structure of disulfide-linked HLA-G dimer. J Biol Chem. 2006;281:10439–10447.

[38] Carosella ED, Rouas-Freiss N, Tronik-Le Roux D, et al. HLA-G: an immune checkpoint molecule. Adv Immunol. 2015;127:33–144.

[39] Manavalan JS, Rossi PC, Vlad G, et al. High expression of ILT3 and ILT4 is a general feature of tolerogenic dendritic cells. Transpl Immunol. 2003;11:245–258.

[40] Lener T, Gimona M, Aigner L, et al. Applying extracellular vesicles based therapeutics in clinical trials - an ISEV position paper. J Extracell Vesicles. 2015;4:30087.

[41] Rebmann V, Konig L, Nardi Fda S, et al. The potential of HLA-G-bearing extracellular vesicles as a future element in HLA-G immune biology. Front Immunol. 2016;7:173.

[42] Alegre E, Rebmann V, Lemaoult J, et al. In vivo identification of an HLA-G complex as ubiquitinated protein circulating in exosomes. Eur J Immunol. 2013;43(7):1933–1939. .

[43] Veit TD, Chies JAB, Switala M, et al. The paradox of high availability and low recognition of soluble HLA-G by LILRB1 receptor in rheumatoid arthritis patients. PLoS One. 2015;10:e0123838.